

Spatial wave intensity correlations in quasi-one-dimensional wires

Gabriel Cwilich,¹ Luis S. Froufe-Pérez,² and Juan José Sáenz²

¹*Department of Physics, Yeshiva University,
500 W 185th Street, New York, NY 10033 USA.*

²*Departamento de Física de la Materia Condensada and Instituto “Nicolás Cabrera”,
Universidad Autónoma de Madrid, 28049 Madrid, Spain*

(Dated: November 23, 2018)

Abstract

Spatial intensity correlations between waves transmitted through random media are analyzed within the framework of the random matrix theory of transport. Assuming that the statistical distribution of transfer matrices is isotropic, we found that the spatial correlation function can be expressed as the sum of three terms, with distinctive spatial dependences. This result coincides with the one obtained in the diffusive regime from perturbative calculations, but holds all the way from quasi-ballistic transport to localization. While correlations are positive in the diffusive regime, we predict a transition to *negative* correlations as the length of the system decreases.

PACS numbers: 42.25.Dd,05.40.-a,72.15.Rn

When a wave propagates coherently through a random medium important correlations emerge between the different propagating paths, which manifest themselves as correlations in the intensity speckle pattern. They have been the subject of great interest over the last decade for the case of temporal, angular, and frequency correlations. [1, 2, 3, 4, 5, 6, 7, 8, 9]. Recently, the direct observation of spatial correlations in the intensity speckle pattern [10, 11] and in the polarization [12] of electromagnetic waves transmitted through a random medium has renewed the interest in this problem [13].

One of the theoretical approaches followed to study this problem involved a microscopic diagrammatic calculation [3, 4, 5]. This was also the approach in the recent work that showed that the spatial correlation function of the normalized intensity can be expressed as the sum of three terms, which differ in their spatial dependence [10], and in the work finding an equivalent structure for the correlations in the polarized radiation [12]. While these diagrammatic approaches have the appealing advantage of illuminating explicitly the nature of the correlations in terms of the microscopic trajectories of the underlying paths, their application is strictly limited to the diffusive regime.

An alternative approach, macroscopic in nature, has been applied successfully to study angular correlations in random media [6, 7, 8, 9] ; it considers the correlations between the transport coefficients in the scattering matrix describing the system in the framework of Random Matrix Theory (RMT) [7, 14, 15]. Most of the work based on RMT has been focused on the study of angular or channel-channel correlations. It shows that only the assumption of isotropy of the transfer matrix distribution, discussed below, determines the structure of the correlations as a function of channel indices. It is the purpose of this work to apply the RMT approach to study the spatial intensity correlation functions. Just from the isotropy condition we derive the structure of the spatial correlations of the normalized intensity. Our result, which coincides with the one obtained from microscopic perturbative calculations (in the diffusive regime)[10] is not perturbative and holds all the way from quasi-ballistic transport to localization. Only the specific values of the three coefficients (C_1 , C_2 and C_3) depend on the transport regime. These values can be obtained from the Monte Carlo solution of the Dorokhov, Mello, Pereyra, and Kumar (DMPK)[14, 16] scaling equation, and are in full agreement with microscopic numerical calculations of bulk disordered wires. While the correlations are positive in the diffusive regime, we predict a transition to *negative* values for both angular and spatial correlations as the length of the system decreases.

We will consider a wave propagating in the z -direction in a constrained geometry (see the inset of Figure 1). The input and output faces of the disordered region are the planes $z = 0$ and $z = L$ respectively. The transverse coordinates in the system are described by $\vec{\rho}$. We will only discuss the case of scalar waves in this work, neglecting polarization effects. The eigenfunctions of the cavity (in the absence of disorder) naturally separate into a longitudinal and a transverse part,

$$\phi_n^\pm(\vec{r}) = \frac{1}{\sqrt{k_n}} \psi_n(\vec{\rho}) \exp\{\pm i k_n z\} \quad (1)$$

The integer $n = 1, 2, \dots, N$ labels the propagating modes, also referred to as scattering channels. Mode n has a real wave number $k_n = \sqrt{k^2 - q_n^2}$, where k is the wavenumber of the incident radiation, and q_n is the momentum associated with the normalized transverse wave function $\psi_n(\vec{\rho})$. The normalization of the total wave function ϕ_n is chosen to carry unit current. The scattering matrix \mathbf{S}

$$\mathbf{S} = \begin{pmatrix} \mathbf{r} & \tilde{\mathbf{t}} \\ \mathbf{t} & \tilde{\mathbf{r}} \end{pmatrix}. \quad (2)$$

relates the asymptotic propagating outgoing waves to the incoming ones: Matrix elements r_{ba} and t_{ja} denote the reflected amplitude in channel b and the transmitted amplitude in channel j when there is a unit flux incident from the left in channel a ; \tilde{r}_{ji} and \tilde{t}_{bi} have an analogous meaning when the incident flux in channel i comes from the right. Flux conservation and reciprocity imply that the matrix \mathbf{S} is unitary and symmetric.

Let us consider two point sources at $\vec{r} = \vec{r}_A$ and $\vec{r} = \vec{r}_B$ on the left hand side of the system, and two detectors at $\vec{r} = \vec{r}_1$ and $\vec{r} = \vec{r}_2$ on the right side (as sketched in Fig. 1). For a point source at $\vec{r} = \vec{r}_A$ the incoming field from the left is proportional to the Green function of the clean waveguide,

$$G_0^+(\vec{r}_A, \vec{r}) = \frac{i}{2} \sum_a \phi_a^{+*}(\vec{r}_A) \phi_a^+(\vec{r}) \quad ; \quad (z > z_A), \quad (3)$$

The field at a point \vec{r}_1 on the right side outside the system will be given by

$$E(A, 1) = \sum_j \left\{ \sum_a t_{ja} c_a \right\} \phi_j^+(\vec{r}_1) \quad (4)$$

where $c_a \propto \phi_a^{+*}(\vec{r}_A)$. The average intensity at that point is given by $\langle I(A, 1) \rangle \equiv \langle |E(A, 1)|^2 \rangle$, where $\langle \dots \rangle$ denotes disorder averaging (over the ensemble of samples). For a finite sample,

the transmission amplitudes, t_{ja} , are assumed to have random phases with $\langle t_{ja} \rangle = 0$ and $\langle t_{ja} t_{j'a'}^* \rangle = \langle T_{ja} \rangle \delta_{aa'} \delta_{jj'}$. The square of the field-field spatial correlation function can be written as

$$C_1(A, 1; B, 2) = \frac{|\langle E(A, 1) E^*(B, 2) \rangle|^2}{\langle I(A, 1) \rangle \langle I(B, 2) \rangle} \quad (5)$$

where

$$\begin{aligned} \langle E(A, 1) E^*(B, 2) \rangle &= \sum_{aa'jj'} c_a d_a^* \phi_j^+(\vec{r}_1) \phi_{j'}^{+*}(\vec{r}_2) \langle t_{ja} t_{j'a'}^* \rangle \\ &= \sum_{aj} c_a d_a^* \phi_j^+(\vec{r}_1) \phi_j^{+*}(\vec{r}_2) \langle T_{ja} \rangle. \end{aligned} \quad (6)$$

(with $d_a \propto \phi_a^+(\vec{r}_B)$). The square of the field-field correlation function takes a simple form in the equivalent channel approximation: Assuming that $\langle T_{ja} \rangle = (1/N^2) \sum_{ja} \langle T_{ja} \rangle \equiv g/N^2$, equation (6) factorizes and

$$C_1(A, 1; B, 2) = |F(\vec{r}_A, \vec{r}_B)|^2 |F(\vec{r}_1, \vec{r}_2)|^2 \quad (7)$$

where $|F(1, 2)|^2$ can be written in terms of the Green function (3):

$$|F(\vec{r}_1, \vec{r}_2)|^2 = \frac{|\Im\{G_0^+(\vec{r}_1, \vec{r}_2)\}|^2}{\Im\{G_0^+(\vec{r}_1, \vec{r}_1)\} \Im\{G_0^+(\vec{r}_2, \vec{r}_2)\}}. \quad (8)$$

In the large- N limit, the Green function of the clean waveguide tends to the free-space Green function, $\exp(ikr)/(4\pi r)$ in the case of a 3D conductor, and we have

$$|F(\vec{r}_1, \vec{r}_2)|^2 \approx \left| \frac{\sin(k|\Delta\vec{r}_{12}|)}{k|\Delta\vec{r}_{12}|} \right|^2 \quad (9)$$

and analogous results holds in 2D with the ‘‘sinc’’ replaced by the Bessel function J_0 :

$$|F(\vec{r}_1, \vec{r}_2)|^2 \approx J_0^2(k|\Delta\vec{r}_{12}|). \quad (10)$$

The behavior of the function $|F|^2$ versus $k\Delta r = k|x_1 - x_2|$ is illustrated in Figure 1. Black dots correspond to the large- N limit, eq. (10). For a finite width, the field correlation function (eq. 8) strongly depends on the position of the detectors. Finite size effects can be minimized by using the experimental approach of ref. [10]: we consider the average of $|F|^2$ when x_1 and x_2 are uniformly distributed over the interval $(W/10, W - W/10)$. As can be seen in Figure 1, the averaged $|F|^2$ (dashed line) already presents the typical large- N behavior for the case of $N = 20$.

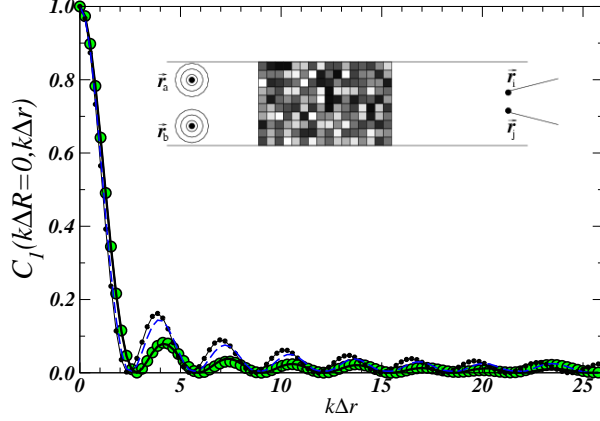


FIG. 1: Square of the field correlation function for a single source as a function of the distance between detectors for a 2D waveguide. The black dots correspond to the expected large- N limit (eq. 10) assuming that all channels are equivalent. For finite N ($N = 20$), the results represent the average over different source and detector positions: The large circles are the results of microscopic numerical calculations (for $g = 1.12$) based on the model system sketched in the inset. The continuous line is the result of equations 5 and 6 with $\langle T_{aj} \rangle$ obtained from the numerical calculations while the dashed line corresponds to the equivalent channel approach, $\langle T_{aj} \rangle = g/N^2$ (eq. 8).

The spatial intensity correlation function can be defined as

$$C(A, 1; B, 2) \equiv \langle I(A, 1)I(B, 2) \rangle - \langle I(A, 1) \rangle \langle I(B, 2) \rangle \quad (11)$$

where the first term of the right hand side is given by

$$\langle I(A, 1)I(B, 2) \rangle = \sum_{aa'bb'} \sum_{ii'jj'} \{ (c_a c_{a'}^* d_b d_{b'}^*) \times (\phi_j^+(\vec{r}_1) \phi_{j'}^{+*}(\vec{r}_1) \phi_i^+(\vec{r}_2) \phi_{i'}^{+*}(\vec{r}_2)) \langle t_{ja} t_{j'a'}^* t_{ib} t_{i'b'}^* \rangle \} \quad (12)$$

In contrast with field-field correlations, the calculation of the averages presents subtle properties directly related to the symmetry and statistical properties of the \mathbf{S} matrix. Calling $\mathcal{T}_1, \mathcal{T}_2, \dots, \mathcal{T}_N$ the set of N common transmission eigenvalues of the four Hermitian matrices $\mathbf{t}\mathbf{t}^\dagger$, $\tilde{\mathbf{t}}\tilde{\mathbf{t}}^\dagger$, $\mathbf{r}\mathbf{r}^\dagger$ and $\tilde{\mathbf{r}}\tilde{\mathbf{r}}^\dagger$, the matrix S can also be written in terms of the \mathcal{T}_n 's by means of the polar decomposition [14, 15]

$$\mathbf{S} = \begin{pmatrix} \mathbf{u}^{(1)} & 0 \\ 0 & \mathbf{u}^{(2)} \end{pmatrix} \begin{pmatrix} -\sqrt{1-\tau} & \sqrt{\tau} \\ \sqrt{\tau} & \sqrt{1-\tau} \end{pmatrix} \begin{pmatrix} \mathbf{u}^{(1)\top} & 0 \\ 0 & \mathbf{u}^{(2)\top} \end{pmatrix}$$

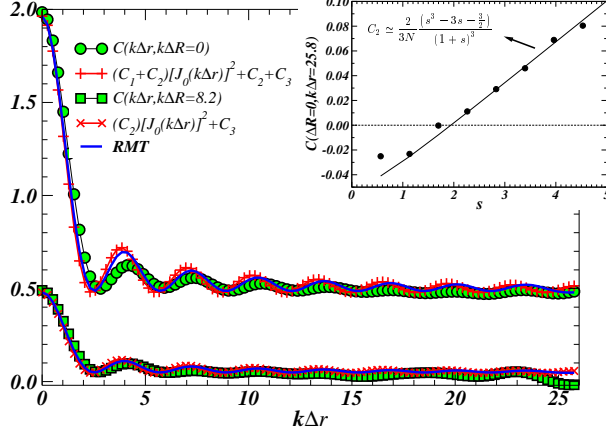


FIG. 2: Plots of the intensity correlation function. Inset: Long range intensity correlations (C_2) as a function of the length $s = L/\ell$ of the system. Black dots are the results of numerical calculations.

where $\mathbf{u}^{(i)}$ are unitary matrices and

$\mathcal{T} = \text{diag}(\mathcal{T}_1, \mathcal{T}_2, \dots, \mathcal{T}_N)$ is a $N \times N$ diagonal matrix with the transmission eigenvalues on the diagonal. The transmission and reflection matrices can, then, be written as

$$r_{ba} = - \sum_n u_{bn}^{(1)} \left(\sqrt{1 - \mathcal{T}_n} \right) u_{an}^{(1)} \quad (13)$$

$$t_{ja} = \sum_n u_{jn}^{(2)} \left(\sqrt{\mathcal{T}_n} \right) u_{an}^{(1)} \quad (14)$$

One of the key assumptions in the macroscopic approach is the hypothesis of *isotropy* [7, 14, 15]. Under this hypothesis the statistical distribution of the transmission eigenvalues $\{\mathcal{T}_n\}$ is independent of the unitary matrices $\mathbf{u}^{(i)}$, and the calculation of the statistical averages in (12) factorizes. Moreover, $\mathbf{u}^{(1)}$ and $\mathbf{u}^{(2)}$ are statistically independent from each other, each being distributed according the invariant measure of the unitary group. By using the averages over the unitary group $\langle (u_{jn})(u_{j'n'})^* \rangle$ and $\langle (u_{jn}u_{im})(u_{j'n'}u_{i'm'})^* \rangle$ (evaluated by Mello in ref. [17]), after some algebra, we find

$$\langle t_{ja} t_{j'a'}^* \rangle = \frac{1}{N^2} \langle T \rangle \delta_{jj'} \delta_{aa'} \quad (15)$$

$$\begin{aligned} \langle t_{ja} t_{j'a'}^* t_{ib} t_{i'b'}^* \rangle = & \\ & [A_N \langle T^2 \rangle - B_N \langle T \rangle^2] (\delta_{ij'} \delta_{i'j} \delta_{ab'} \delta_{a'b} + \delta_{jj'} \delta_{ii'} \delta_{aa'} \delta_{bb'}) \\ & + [A_N \langle T \rangle^2 - B_N \langle T \rangle] (\delta_{jj'} \delta_{ii'} \delta_{ab'} \delta_{a'b} + \delta_{ij'} \delta_{i'j} \delta_{aa'} \delta_{bb'}) \quad (16) \end{aligned}$$

introducing the notation $g = \langle T \rangle \equiv \sum_n \langle \mathcal{T}_n \rangle$,

$\text{var}\{g\} \equiv \langle T^2 \rangle - \langle T \rangle^2$, $\langle T_2 \rangle \equiv \sum_n \langle \mathcal{T}_n^2 \rangle$ and the coefficients A_N and B_N given by

$$A_N = \frac{N^2 + 1}{N^2} \frac{1}{(N^2 - 1)^2} \quad ; \quad B_N = \frac{2}{N} \frac{1}{(N^2 - 1)^2}$$

From equation (16), and taking $i = i', j = j'$,

$a = a', b = b'$, we easily recover the well known channel-channel correlation function C_{jaib} [6]

$$\frac{\langle T_{ja} T_{ib} \rangle}{\langle T_{ja} \rangle \langle T_{ib} \rangle} - 1 = C_1 (\delta_{ij} \delta_{ab}) + C_2 (\delta_{ab} + \delta_{ij}) + C_3 \quad (17)$$

where

$$C_1 \equiv \frac{N^4}{\langle T \rangle^2} [A_N \langle T^2 \rangle - B_N \langle T_2 \rangle] \quad (18)$$

$$C_2 \equiv \frac{N^4}{\langle T \rangle^2} [A_N \langle T_2 \rangle - B_N \langle T^2 \rangle] \quad (19)$$

$$C_3 \equiv C_1 - 1 \quad (20)$$

The angular correlation function has the same structure as that found first by Feng *et al.* [5], the three coefficients C_1 , C_2 and C_3 corresponding, respectively, to short, long and infinite range correlations.

In order to obtain the spatial correlation function, we substitute the expressions (15) and (16) for the averages in equations (6) and (12),

$$\begin{aligned} C(\Delta \vec{r}_{ab}, \Delta \vec{r}_{12}) &\equiv \frac{\langle I(a, 1) I(b, 2) \rangle}{\langle I(a, 1) \rangle \langle I(b, 2) \rangle} - 1 = \\ &C_1 (|F(\vec{r}_a, \vec{r}_b)|^2 |F(\vec{r}_1, \vec{r}_2)|^2) \\ &+ C_2 (|F(\vec{r}_a, \vec{r}_b)|^2 + |F(\vec{r}_1, \vec{r}_2)|^2) + C_3 \end{aligned} \quad (21)$$

where $|F(1, 2)|^2$ is the square of the field correlation function (eq. 8) and the correlation coefficients C_1 , C_2 and C_3 are *exactly the same* as those appearing in equation (17). The structure of the spatial correlations is, then, equivalent to that obtained for channel correlations with the angular “ δ_{ab} ” functions replaced by the spatial functions $|F(a, b)|^2$.

The behavior of the spatial correlations is illustrated in Figure 2. For a single source and two detectors ($\Delta \vec{r}_{ab} = \Delta R = 0$ and $\Delta \vec{r}_{12} \equiv \Delta r$), or viceversa, the correlation function (in a 2D waveguide) is given by $\approx (C_1 + C_2)(J_0(k\Delta r))^2 + C_2 + C_3$ and approach a constant as Δr increases. For large ΔR , the correlations as a function of Δr behave as $\approx C_2(J_0(k\Delta r))^2 + C_3$. These results are in qualitative agreement with the results of reference [10]. As a

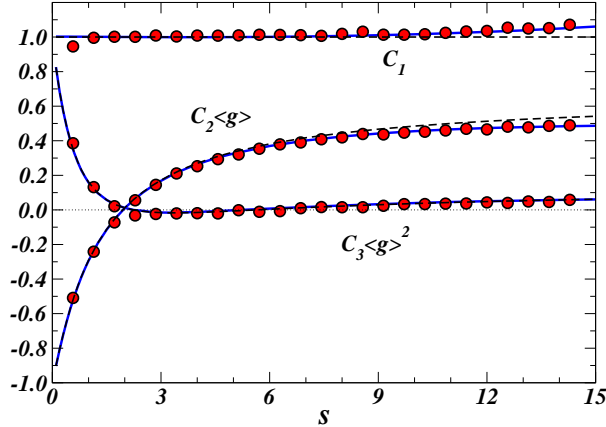


FIG. 3: Correlation coefficients C_1 , C_2 and C_3 as a function of the length $s = L/\ell$ of the system. Continuous lines are the results of the DMPK equation. Dashed line represents the perturbative $1/N$ expansion (after ref. [9]). Circles are numerical results for the model system sketched in Fig. 1

matter of fact, our expressions (21) and (8) (or 9 in the large- N limit) are consistent, after a slight reordering of the terms, with the expression (5) in reference [10], which was obtained through a perturbative diagrammatic expansion. The equivalence with polarization correlations (equation (2) of reference [12]) is also evident. However, while the diagrammatic expansions are strictly valid in the diffusive regime, our result **does not depend at all on the transport regime**, and are a direct consequence of the isotropy hypothesis. Only the relative *size* of C_1 , C_2 and C_3 will depend on the length of the system L and the mean free path ℓ through the distribution of transmission eigenvalues $P(\{\mathcal{T}_n\}, s)$, with $s = L/\ell$. Figure 3 summarizes the dependence of the correlation coefficients with the length of the system as obtained from a Monte Carlo calculations of the DMPK equation [18]. In the diffusive regime ($1 \ll g \ll N$), the correlation factors take the well known values [5, 6]: $C_1 \approx 1$, $gC_2 \approx 2/3$ and $g^2C_3 \approx 2/15$. As the length of the system decreases the exact solution of the DMPK equation is well described by the known analytical results based on $1/N$ expansion [9] (dashed line in Fig. 3). While the correlations are positive in the diffusive regime, our results predict *a transition to negative correlations for both the angular and the spatial case* (see inset in Fig. 2).

In order to confirm the predictions of the macroscopic approach, we have performed extensive numerical calculations based on the simple two-dimensional (2D) model sketched in Fig. 1. For electromagnetic waves, we assume s-polarization with the electric vector

parallel to the walls. The disordered region is divided in small rectangular regions of section $\delta_z \times \delta_x$. Within each slice the refraction index n_R has random values distributed uniformly in the interval $(1 - \delta n_R, 1 + \delta n_R)$. We take $\delta_x = W/10$, $\delta_z = W/20$ and $\delta n_R = 0.025$, for a 20-mode waveguide ($W/\lambda = 10.25$) as in Figure 1. Transmission and reflection coefficients are exactly calculated by solving the 2D wave equation by mode matching at each δ_z -slice, together with a generalized scattering-matrix technique [19]. Figure 1 shows the behavior of the averaged field correlations (for $s = 15$, $\langle g \rangle = 1.12$). The numerical results show that transport is not fully isotropic (the distribution of the transmission coefficients T_{ja} has some dependence on the particular values of j and a). The numerical intensity correlations are very close to the expected behavior (see Fig. 2) although they are not fully described by equations 17 and 21. However we can extract the correlation coefficients C_1, C_2 and C_3 from a least square fitting of spatial or angular numerical correlations with equation (21) or (17) respectively. In both cases, the obtained coefficients (circles in Figure 3) are in full agreement with the predictions of the DMPK approach.

This work has been supported by the Spanish MCyT (Ref. No. BFM2003-01167) and the European Integrated Project "Molecular Imaging" (LSHG-CT-2003-503259). One of us (GC) wants to acknowledge the hospitality of the D.F.M.C. (U.A.M. - Spain) where this work was completed.

-
- [1] *Waves and Imaging through Complex Media*, ed. by P. Sebbah, (Kluwer, Dordrecht 2001).
 - [2] *Wave Scattering in Complex Media: From Theory to Applications*, ed. by B. van Tiggelen and S. Skipetrov, (Kluwer, Dordrecht 2003).
 - [3] I. Freund, M. Rosenbluh and S. Feng, Phys. Rev. Lett. **61**, 2328 (1988)
 - [4] M. J. Stephen and G. Cwilich, Phys. Rev. Lett. **59**, 285 (1987)
 - [5] S. Feng *et al.*, Phys. Rev. Lett. **61**, 834 (1988)
 - [6] P.A. Mello, E. Akkermans and B. Shapiro, Phys. Rev. Lett. **61**, 459 (1988)
 - [7] P.A. Mello and A. D. Stone, Phys. Rev. **B44**, 3559 (1991).
 - [8] E. Bascones *et al.*, Phys. Rev. B **55**, R11911 (1997).
 - [9] A. García-Martín *et al.*, Phys. Rev. Lett. **88**, 143901 (2002); J.J. Sáenz, L.S. Froufe-Pérez and A. García-Martín, in reference [2], page 175.

- [10] P. Sebbah *et al.*, Phys. Rev. Lett **88**, 123901 (2002).
- [11] V. Emiliani *et al.*, Phys. Rev. Lett. **90**, 250801 (2003).
- [12] A.A. Chabanov *et al.*, Phys. Rev. Lett **92** 173901 (2004).
- [13] Y.H. Kim *et al.*, Phys. Rev. Lett. **94**, 036804 (2005); S. E. Skipetrov, *ibid.* **93**, 233901 (2004);
A. A. Chabanov *et al.*, *ibid.* **93**, 123901 (2004); V. M. Apalkov *et al.*, *ibid.* **92**, 253902 (2004).
- [14] P.A. Mello, P. Pereyra, and N. Kumar, Ann. Phys. (N.Y.) **181**, 290 (1988).
- [15] C.W.J. Beenakker, Rev. Mod. Phys. **69**, 731 (1997).
- [16] O.N. Dorokhov, Solid State Commun. **51**, 381 (1984)
- [17] P.A. Mello, J. Phys. **A 23**, 4061 (1990).
- [18] L.S. Froufe-Pérez *et al.*, Phys. Rev. Lett. **89**, 246403 (2002).
- [19] J. A. Torres and J. J. Sáenz, Jap. J. Appl. Phys. **73**, 2182 (2004).